

Quantum versus classical angular momentum

Jan Mostowski¹  and Joanna Pietraszewicz¹

Institute of Physics of the Polish Academy of Sciences, Al. Lotników 32/46, 02-668 Warszawa, Poland

E-mail: mosto@ifpan.edu.pl and pietras@ifpan.edu.pl

Received 22 July 2019, revised 16 September 2019

Accepted for publication 4 October 2019

Published 16 January 2020



CrossMark

Abstract

Angular momentum in classical mechanics is given by a vector. The plane perpendicular to this vector, in accordance to central field theory, determines the space in which particle motion takes place. No such simple picture exists in quantum mechanics. The states of a particle in a central field are proportional to spherical harmonics which do not define any plane of motion. In the first part of this paper we discuss the angular distribution of particle position and compare it to the classical probabilistic approach. In the second part, the matter of addition of angular momenta is discussed. In classical mechanics this means addition of vectors, while in quantum mechanics Clebsch–Gordan coefficients have to be used. We have found classical approximations to quantum coefficients and the limit of their applicability. This analysis gives a basis for the so-called ‘vector addition model’ used in some elementary textbooks on atomic physics. It can help to better understand the addition of angular momenta in quantum mechanics.

Supplementary material for this article is available [online](#)

Keywords: angular momentum, classical limit of quantum mechanics, Clebsch–Gordan coefficients

(Some figures may appear in colour only in the online journal)

1. Introduction

Angular momentum in classical mechanics measures the ‘amount of rotation’. In a sense, it is analogous to linear momentum, which measures the ‘amount of motion’. The exact definition

¹ Authors to whom any correspondence should be addressed.

of angular momentum is usually given in undergraduate physics courses. For a point particle, it is defined as the cross product of the position and momentum vectors. A standard reasoning leads to the conservation law, according to which angular momentum is conserved for motion in a central field. The particle motion then becomes restricted to a plane perpendicular to the angular momentum vector.

Turning now to quantum mechanics, one needs operators representing physical quantities and states (wavefunctions) specifying the system. Angular momentum is the physical quantity considered in this paper. Operators representing this quantity are defined as the cross product of position and momentum operators. Of course, the angular momentum is conserved for central interactions—as in classical mechanics. Unlike in classical mechanics, the plane of motion is not uniquely specified.

Note also that no quantum state can be a common eigenstate of all three vector components of angular momentum. In turn, common eigenstates of one of its components, usually the z one, and of the total angular momentum, exist and are routinely used in the description of systems with spherical symmetry. Eigenstates having maximal and minimal values of the z component of angular momentum, i.e. equal to the total angular momentum j or $-j$, correspond to motion in the xy plane. This property is stated in some textbooks [1], and educational papers [2]. In our approach we also use this fact. States with other values of z component are much more difficult to interpret.

Careful inspection of eigenfunctions of the total angular momentum and the z component (spherical harmonics) and their dependencies on angles in spherical coordinates is the key to understand angular momentum. Any confusion at this stage makes it impossible to find any resemblance between these quantum states and more familiar quantities known from classical mechanics, e.g. the plane of motion. Thus, the quantum–classical correspondence for angular momentum states remains unclear to many students.

Addition of angular momenta is also a confusing topic. In classical mechanics it is very simple: two vectors of angular momenta should be added to get the total angular momentum. The corresponding case in quantum mechanics is not trivial, so standard textbooks do not present this topic at sufficient depth. Instead, the explanation is reduced to information that addition of angular momenta requires introduction of Clebsch–Gordan coefficients. Explicit formulas for them are usually restricted to small values of angular momentum, while the relation to the addition of classical angular momenta is not discussed at all.

In the present paper we apply and adapt classical probabilistic models that mimic quantum states with a given angular momentum. These models originate from the so-called ‘vector model’ of angular momentum, used in some textbooks on atomic physics [3–5]. As opposed to these textbooks, we provide a thorough discussion of these models, compare them with a full quantum mechanical treatment and discuss their range of applicability. In this way the relation between the classical and quantum approaches to angular momentum will be established and visualized. Classical models are also supported by semiclassical (WKB) approximations to the angular momentum states.

One should realize that the joining platform for studies of quantum–classical quantities’ correspondence is the limit of large values of measurable quantities. With this assumption the quantum system becomes similar to its classical counterpart, although it retains quantum features. For example, it can be found in various states with some probability amplitude.

In this paper we investigate addition of angular momenta, with the help of the classical probabilistic approach and comparing the results with the quantum case. All these will help students to understand the relation between classical vector addition of angular momentum and the corresponding quantum case.

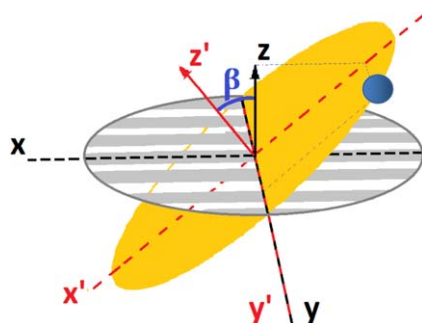


Figure 1. The trajectory of a particle lies in the x' , y' plane. The angular momentum vector is perpendicular to the plane of motion, hence directed along the z' axis, which forms angle β with the z axis of the laboratory coordinate frame. The y axis in the laboratory frame and the y' axis in the plane of motion are common for both frames. The dotted blue lines show the projection of particle position on the x' and y' axes.

We should also mention that quantum systems with large angular momenta have become a subject of increasing studies in recent years, e.g. [6–8]. A deep understanding of these states and their relation to classical physics seems to be becoming an important part of an advanced physics education. The probabilistic approach presented here can be used in courses on quantum mechanics at the graduate level. The results presented should help students to better understand this element of quantum mechanics.

2. Classical approach to angular momentum

We will begin with a formulation of purely classical motion and classical angular momentum. A scheme of the classical system is roughly shown in figure 1. Consider a point particle with mass μ undergoing circular motion in a plane (orange one in figure 1). Orientation of the plane is characterized by the angular momentum vector (red arrow in figure 1), which forms angle β with the z axis.

It is important to describe the particle motion by giving the time dependence of its coordinates. In the plane of motion, i.e. perpendicular to the angular momentum, the motion is given by $x'(t) = r \cos(\omega t + \alpha)$, $y'(t) = r \sin(\omega t + \alpha)$, where x' and y' are in-plane coordinates, and r is the radius of the orbit. Angle α denotes the initial phase of the motion.

In order to find particle coordinates in the laboratory frame (gray plane in figure 1), one has to rotate the coordinate system around the y axis by angle β . After such rotation one gets

$$x(t) = x'(t) \cos \beta = r \cos(\omega t + \alpha) \cos \beta \quad (1)$$

$$y(t) = y'(t) = r \sin(\omega t + \alpha) \quad (2)$$

$$z(t) = x'(t) \sin \beta = r \cos(\omega t + \alpha) \sin \beta. \quad (3)$$

The system together with coordinates is presented in figure 1.

The angular momentum value L is related to the parameters r and ω by the formula $L = \mu r^2 \omega$, and the value of the z component of angular momentum is $L_z = \mu r^2 \omega^2 \cos \beta$.

In the next section the classical description of angular momentum will be the subject of comparison with the quantum description. For both cases we will calculate the probability density that the \vec{r}' forms angle θ with the z axis. At first, however, we have to introduce a

probabilistic approach to the classical theory, since this is required by quantum mechanics. After all, we want to draw conclusions for analogy of the same quantity.

We introduce an ensemble of particles to classical theory. The motion of each particle is characterized by α , which is a random variable with uniform distribution in the range $[0, 2\pi]$. The quantity we are looking for has the following definition:

$$p(\cos \theta) = \frac{1}{2\pi} \int_0^{2\pi} d\alpha \delta\left(\cos \theta - \frac{z(t)}{r}\right), \quad (4)$$

where $\delta(Z)$ is the Dirac delta function. Note that argument Z depends on t and α as well. Inserting the value of $z(t)$ from equation (3) and integrating over α , we get

$$p(\cos \theta) = \frac{1}{2\pi} \frac{1}{\sqrt{\cos^2 \theta - \sin^2 \beta}} \text{ in the 'allowed range' } |\cos \theta| > |\sin \beta|, \quad (5)$$

or $p(\cos \theta) = 0$ for $\cos \theta$ outside the 'allowed' range. For details of the derivation we refer readers to the [appendix](#). Further discussion of the function $p(\cos \theta)$ will be given in the next section.

3. Angular momentum in quantum mechanics

Description of any physical system in the framework of quantum mechanics requires information about the state of the system, and about relevant physical quantities represented by linear operators. In this paper the relevant physical quantities are components of angular momenta. We will not consider any other physical quantities.

Angular momentum operators J_x , J_y , and J_z obey commutation relations:

$$[J_\sigma, J_\nu] = i\hbar \epsilon_{\sigma\nu\kappa} J_\kappa, \quad (6)$$

where $\epsilon_{\sigma\nu\kappa}$ is a purely antisymmetric unit tensor. The states of the system can be chosen as common eigenstates of the operator $J^2 = J_x^2 + J_y^2 + J_z^2$ (with eigenvalues $\hbar^2 j(j+1)$, where $j = 0, 1, \dots$) and operator J_z (with eigenvalues $\hbar m$, where $m = -j, -j+1, \dots, j$). These states are denoted by $|j, m\rangle$.

Observe that two other components of the angular momentum, J_x and J_y , do not have well-defined values in states $|j, m\rangle$. Their average values are equal to zero, whereas their dispersions are equal to

$$\Delta^2 J_x = \Delta^2 J_y = \frac{\hbar^2}{2} (j(j+1) - m^2). \quad (7)$$

States with $m = \pm j$ have the smallest dispersion. States with $m = 0$ have the largest dispersion, comparable to j .

Angular momentum operators are often considered in the position representation:

$$J_\sigma = \frac{\hbar}{i} \epsilon_{\sigma\nu\kappa} x_\nu \frac{\partial}{\partial x_\kappa}, \quad (8)$$

where x_κ , with $\kappa = 1, 2, 3$, denoting Cartesian coordinates. In this representation the eigenstates of both operators J^2 and J_z are given by a combination of spherical harmonics $Y_{j,m}(\theta, \varphi)$ ². There are many different phase conventions for $Y_{j,m}(\theta, \varphi)$. We have adopted the phase convention used in Mathematica.

² The eigenstates of both operators J^2 and J_z in the position representation are given by spherical harmonics $Y_{j,m}(\theta, \varphi)$.

The explicit form of spherical harmonics can be found in many textbooks, so we will not reproduce them here. We will, however, mention a peculiar feature possessed by spherical harmonics $Y_{j,j}(\theta, \varphi)$. Since they are proportional to $\sin^j(\theta) \exp(i j \varphi)$, they strongly concentrate around $\theta \approx \pi/2$ in the limit of large j . This is an argument for treating $Y_{j,j}(\theta, \varphi)$ as a state which is an analogue of classical motion in the $\theta = 0$, and hence in the xy , plane [1, 2]. Other spherical harmonics do not have this property. They are not concentrated in a plane and, moreover, they exhibit oscillations with θ . One of the aims of the paper is to provide a classical interpretation for these states.

Absolute values squared of some spherical harmonics are shown in figure 2. In addition, their semiclassical (WKB) approximation valid for large j are also given. For details of the semiclassical approximation, see the supplementary material (S1 available online at stacks.iop.org/EJP/41/025402/mmedia).

Semiclassical approximation is introduced here to give the feeling of the overall behavior of spherical harmonics. If one interprets j classically as the total angular momentum, and m as its z component, then the classical motion is restricted to the interval $\sin \theta \geq \frac{|m|}{j}$. Thus, ‘classical turning points’ should exist also in the quantum case. One can clearly identify these points in case of large j and m in figure 2—spherical harmonics decay to zero beyond such θ that $m^2 \approx j^2 \sin^2 \theta$ and exhibit oscillations in the ‘classically allowed region’ between these points. The period of these oscillations scales with j as j^{-1} .

The modulus square of the spherical harmonics $|Y_{j,m}(\theta, \varphi)|^2$ one can interpret as the probability density of finding a particle with quantum numbers j and m at the angle θ . This probability density can be compared to a purely classical result, namely equation (5), which gives the classical probability distribution of angles. Firstly, we see that the classical distribution mimics the quantum one in case of large j . Rapid oscillations that are present in the quantum case and absent in the classical distribution are exceptions. Secondly, we see that the classical approximation gives the average over several oscillations of the quantum result. In other words, the classical approach is valid if the resolution of the measuring device does not allow one to measure high-frequency oscillations.

One should bear in mind, however, that the classical angular momentum is a continuous variable as opposed to the quantum case. We have identified the classical value of L with the quantum value $\hbar j$, and the classical L_z with the magnetic quantum number m multiplied by \hbar , although whole ranges of L and of L_z , with lengths comparable to \hbar , approximate equally well the quantum case.

4. Addition of angular momenta

We will begin by discussing addition of angular momenta in classical mechanics. Consider two spinning tops, one with angular momentum \mathbf{L}_1 , the other with angular momentum \mathbf{L}_2 . The total angular momentum of the system is thus $\mathbf{L} = \mathbf{L}_1 + \mathbf{L}_2$. The length of the total angular momentum is $L = \sqrt{L_1^2 + L_2^2 + 2 L_1 L_2 \cos \alpha}$, where L_1 and L_2 denote lengths of the appropriate vectors and α is the angle between them. The range of L values extends between $|L_1 - L_2|$ and $(L_1 + L_2)$, depending on the angle α between the two vectors. The direction of the total angular momentum can be easily found with the help of vector addition.

We will turn now to quantum mechanics. Consider two subsystems, one in the state $|j_1, m_1\rangle$ and the second one in the state $|j_2, m_2\rangle$. These states belong to different spaces, so the space of states of the combined system is the (tensor) product of two spaces. Among all states of the whole system, one can distinguish product states $|j_1, m_1\rangle |j_2, m_2\rangle$. The meaning of these

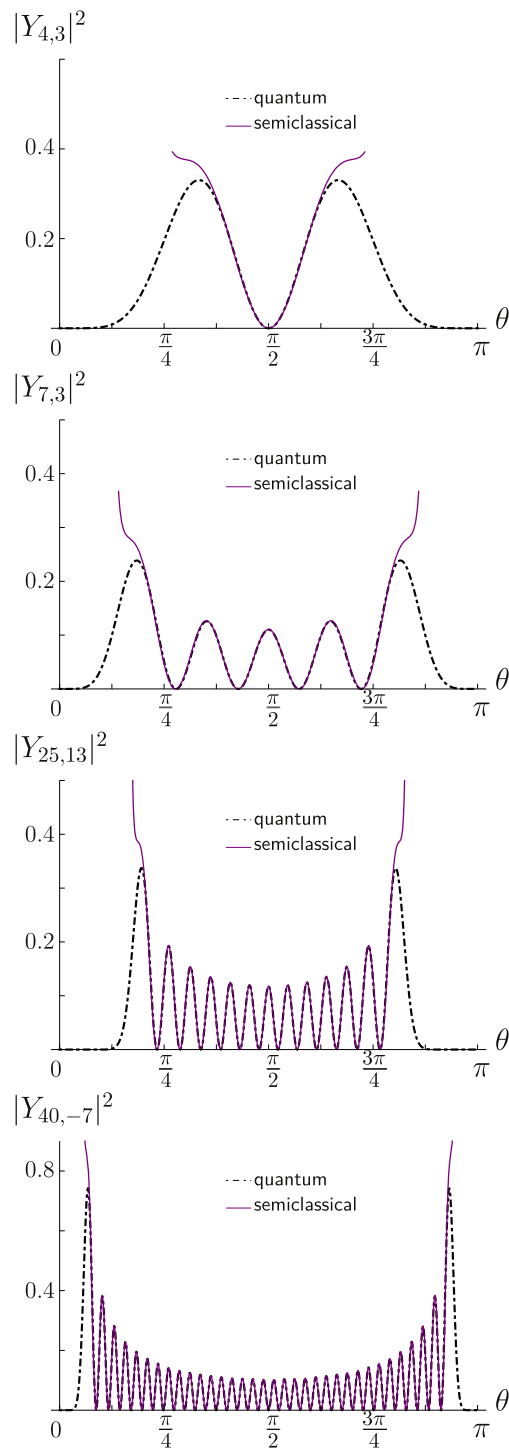


Figure 2. Spherical harmonic squared $|Y_{j,m}(\theta, \varphi)|^2$ versus angle θ (the modulus square does not depend on φ) are presented for quantum solution (black, dot-dashed line) and for its semiclassical counterpart (purple, solid line). Values j and m are on the plot.

states is that the first subsystem is in the $|j_1, m_1\rangle$ state and the second subsystem in the $|j_2, m_2\rangle$ state.

The total angular momentum operator is defined, as in classical physics, by the sum of individual components, $J_\sigma = J_{1\sigma} + J_{2\sigma}$, where $\sigma = x, y, z$. The operators $J_{1\sigma}, J_{2\sigma}$ satisfy the same commutation relations as the individual components; see equation (6).

The product states are not, in most cases, eigenstates of the square of the total angular momentum $\mathbf{J}^2 = J_x^2 + J_y^2 + J_z^2$, but they are definitely eigenstates of $J_{1z} + J_{2z}$. One can find, however, states in the product space which are eigenstates of both \mathbf{J}^2 and J_z . They are denoted by $|J, M\rangle$ and are, of course, linear combinations of the product states

$$|J, M\rangle = \sum_{m_1, m_2} \text{CB}(j_1, m_1, j_2, m_2; J, M) |j_1, m_1\rangle |j_2, m_2\rangle. \quad (9)$$

Coefficients $\text{CB}(j_1, m_1, j_2, m_2; J, M) = \text{CB}$ are called Clebsch–Gordan coefficients. Explicit formulas for them can be found in some textbooks, but these formulas are not very useful and will not be reproduced here. Values of $\text{CB}(j_1, m_1, j_2, m_2; J, M)$, when needed, can be found in quantum mechanics textbooks or in easily available tables. Some symbolic computer languages, like Mathematica, have build-in procedures to find their values.

We have to bear in mind that Clebsch–Gordan coefficients are probability amplitudes and that there is no way to define their phases in an unambiguous way. Most, if not all, textbooks use the so-called Shockley convention, where all coefficients are real while their signs are fixed.

Explanation of the overall behavior of the CB coefficients based on a classical model will be given in the next section.

5. Classical and quantum Clebsch–Gordan coefficients

We will adopt and apply a classical probabilistic model of addition of two angular momenta and compare the results with the exact quantum values.

The classical model is supposed to mimic addition of quantum angular momenta. The quantum $|j, m\rangle$ states that will be superimposed and their angular momenta added, have a well-defined total angular momentum and the z component of angular momentum, while the other two components are random—loosely speaking. This gives an inspiration for using the classical probabilistic approach, formulated below.

The classical limit of Clebsch–Gordan coefficients was found by E Wigner with the method outlined in [9]. (Strictly speaking, Wigner considered $3j$ symbols rather than Clebsch–Gordan coefficients, but the difference between them is marginal.) In Wigner’s approach one considers two vectors and their sum. The components of the sum can have different orientations in space. A simplified derivation of the classical limit of $3j$ symbols is given under the assumption that the vectors being added undergo a uniform motion around the z axis. This mimics a random orientation of vectors. In the next part we will provide a formal derivation of essentially the same result.

Let us assume that the classical angular momentum vector \mathbf{L}_1 has components

$$\begin{aligned} L_{1,x} &= L_1 \sin \theta_1 \cos \varphi_1, \\ L_{1,y} &= L_1 \sin \theta_1 \sin \varphi_1, \\ L_{1,z} &= L_1 \cos \theta_1. \end{aligned}$$

The components of the second vector \mathbf{L}_2 are

$$\begin{aligned} L_{2,x} &= L_2 \sin \theta_2 \cos \varphi_2, \\ L_{2,y} &= L_2 \sin \theta_2 \sin \varphi_2, \\ L_{2,z} &= L_2 \cos \theta_2. \end{aligned}$$

Angles θ_1 and θ_2 define the z components of both angular momenta and are assumed to be fixed. Angles φ_1 and φ_2 , defining the x and y components of angular momenta, are assumed to be random variables with an uniform distribution.

We will now find the probability distribution of the square of the total angular momentum. It is given by the average value of the δ function over possible angle settings:

$$p(L^2) = \frac{1}{(2\pi)^2} \int d\varphi_1 d\varphi_2 \delta(L^2 - L_1^2 - L_2^2 - 2L_1L_2 \cos \alpha). \quad (10)$$

The angle α between the vectors can be expressed in terms of θ_1 , θ_2 , φ_1 and φ_2 :

$$\cos \alpha = \cos \theta_1 \cos \theta_2 + \sin \theta_1 \sin \theta_2 \cos(\varphi_1 - \varphi_2). \quad (11)$$

Inserting equation (11) into equation (10), we get

$$p(L^2) = \frac{1}{2\pi} \int d\varphi \delta(L^2 - L_1^2 - L_2^2 - 2L_1L_2(\cos \theta_1 \cos \theta_2 + \sin \theta_1 \sin \theta_2 \cos(\varphi_1 - \varphi_2))). \quad (12)$$

Integration over φ_1 and φ_2 gives

$$p(L^2) = \frac{1}{\pi} \frac{1}{\sqrt{(L_1^2 + L_2^2 + 2L_1L_2 \cos(\theta_1 + \theta_2) - L^2)(L^2 - L_1^2 - L_2^2 - 2L_1L_2 \cos(\theta_1 - \theta_2))}}. \quad (13)$$

Finally, the distribution of L can be obtained with the help of the relation

$$p(L) = 2L p(L^2). \quad (14)$$

Details of calculations leading to the formulas given above can be found in the [appendix](#).

To make the quantum–classical correspondence even more readable, we have to interpret angles θ_1 and θ_2 . Interpretation should be just like in quantum mechanics, i.e. the projection of the angular momentum on the z axis is equal to the magnetic quantum number m . Therefore, $L_{z_1} = L_1 \cos \theta_1$, $L_{z_2} = L_2 \cos \theta_2$ and $L_z = L_{z_1} + L_{z_2}$, which allows ones to write

$$\begin{aligned} p(L) &= \frac{1}{\pi} \frac{2L}{\sqrt{\mathcal{A}^2 + 4[L^2 L_{z_1} L_{z_2} - (L_2^2 L_{z_1} + L_1^2 L_{z_2})L_z]}} \\ \mathcal{A}^2 &= -L^4 - L_1^4 - L_2^4 + 2L^2(L_1^2 + L_2^2) + 2L_1^2 L_2^2. \end{aligned} \quad (15)$$

The above probability distribution $p(L)$ should be understood as the classical equivalent of the CG coefficient squared. We have got, therefore, a classical analogue of the Clebsch–Gordan coefficients.

Numerical values of the quantum mechanical Clebsch–Gordan coefficients are easily available. We used Mathematica to get their values and to plot their absolute values squared, as is shown in figures 3 and 4.

We will now compare the classical distribution of the total angular momentum with squares of the Clebsch–Gordan coefficients. We should stress that the classical angular momentum is a continuous quantity, whereas the quantum angular momentum is discrete.

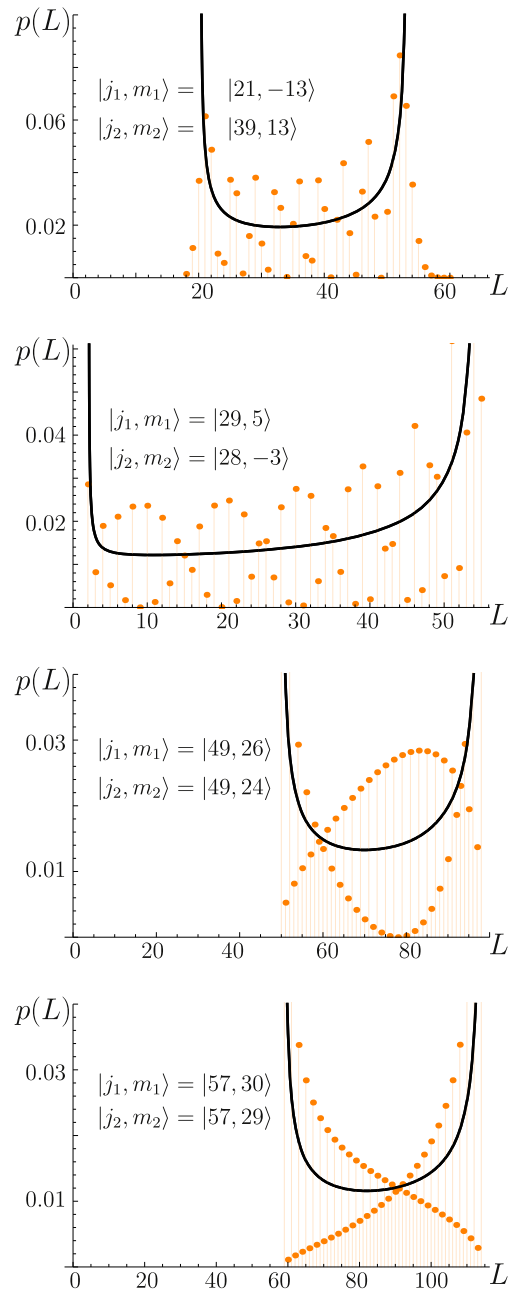


Figure 3. Probability distribution of the total angular momentum (equivalent to the probability of the azimuth angle). The orange points denote values of the squares of Clebsch–Gordan coefficients that fulfill conditions imposed by the quantum numbers j_1, m_1, j_2, m_2 . Their values are shown in each plot. The solid lines are classical results.

We have, therefore, to introduce a finite interval dL of the continuous variable L . The probability density $p(L)$ multiplied by dL should be compared with the quantum probability $p(J)$. A possible choice in our case, and the easiest one, is to take $dL = \hbar$ (the Planck constant). This allows one to

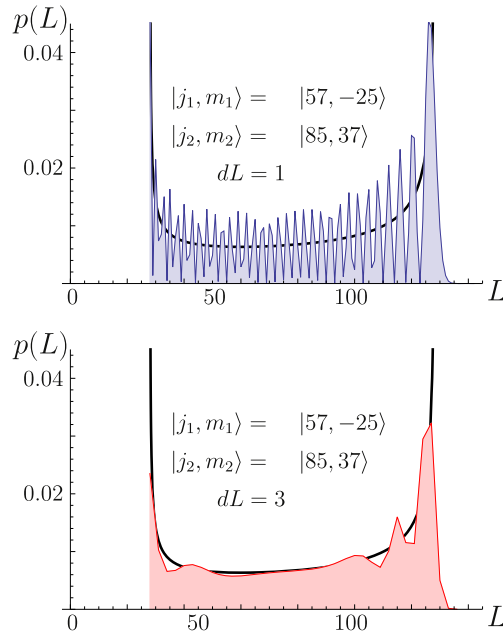


Figure 4. The role of the resolution of the measuring device in allowing/preventing accurate detection of values of the Clebsch–Gordan coefficients (values of quantum numbers are given in the plot). If the resolution dL (in units of \hbar) is such that $dL \lesssim 1$, then the classical model does not reproduce the quantum values (upper plot). In case $dL \gtrsim 1$ (lower plot), the quantum values, averaged over dL , are well reproduced by the classical model.

make a direct comparison of squares of the Clebsch–Gordan coefficients and classical probability distribution of the total angular momentum.

It is seen from the plots that the classical probability distribution reproduces the general character of the quantum Clebsch–Gordan coefficients. This takes place even for relatively small values of angular momenta. Of course, the classical approach gives probabilities, as opposed to the quantum version, which gives probability amplitudes, and hence relative phases of the coefficients in addition to their absolute values.

However, there are examples (shown by the black solid line in figure 3), where the classical values do not represent properly the quantum values. This is due to their oscillations with a large amplitude and frequency equal to one unit of angular momentum \hbar . This does not mean that the classical approximation fails in these cases. This is one more illustration of the fact that the classical approximation gives average values only. If measurements of the angular momentum are precise enough to distinguish between values of L that differ by \hbar , then differences between classical and quantum values can be found. If, however, the resolution is insufficient to detect values that differ by \hbar then the classical picture suffices to describe the system.

This effect is illustrated in figure 4, where two angular momenta, $j_1 = 57$, $m_1 = -25$ and $j_2 = 85$, $m_2 = 37$, are added. The dependence of the Clebsch–Gordan coefficients squared as functions of the total angular momentum are shown. The solid line represents the classical distribution given by equation (15). If the resolution of measurement of the total

angular momentum is 1 (meaning one quantum unit, hence \hbar), then the classical distribution differs from the quantum one. If, however, the resolution is $dL = 3$, as shown in the right panel, the averaged quantum results are very close to the classical ones. Further discussion of this matter is given in the supplementary material (S2).

6. Conclusions

We have discussed a classical interpretation of the Clebsch–Gordan coefficients, valid for large values of all three angular momenta involved. We have shown that in some cases the classical model gives a good approximation to the exact quantum values. This behavior is in fact expected.

The unexpected, in turn, was an appearance of conditions that are needed for the classical approach and the classical vector addition model to be valid. If these conditions are not fulfilled, the classical vector addition model can be insufficient to find approximate values of the Clebsch–Gordan coefficients. This is most pronounced when the two added angular momenta have similar values. In this case, Clebsch–Gordan coefficients exhibit rapid oscillations in the total angular momentum. These oscillations cannot be explained by any kind of classical model.

Our results illustrate an interesting, but known, feature of the classical limit of quantum mechanics. Not only should all relevant physical quantities have large values (large as compared to their single quantum units, like \hbar in the studied case of angular momentum), but measurements of these physical quantity have to be taken into account as well. Quantum physics has to be used to describe the results of measurements with resolution better than \hbar , whereas classical physics only describes measurements that average over intervals of angular momentum that are larger than the quantum unit.

This paper has shown aspects of angular momentum and addition of angular momenta that can be approximately described in the framework of classical physics. The analysis presented here should provide better understanding of quantum angular momentum physics. Classical analogues cannot, of course, explain quantum effects. They can, however, illustrate some general features of the system and their relation to classical physics.

Appendix—Derivation of some formulas involving the Dirac delta function

In this appendix we will prove the correctness of equation (4), equation (10) and equation (14).

A1. Calculation of integrals involving the Dirac delta function

The integral to be calculate is

$$I_1(a, b) = \int_0^\pi d\xi \delta(a - b \cos \xi). \quad (16)$$

Note that the expression in equation (4) is roughly of this kind. By definition of the Dirac delta function, the following rules apply:

$$\int_{x_1}^{x_2} dx f(x) \delta(a - x) = f(a) \quad (17)$$

if $x_1 < a < x_2$, or

$$\int_{x_1}^{x_2} dx f(x) \delta(a - x) = 0 \quad (18)$$

otherwise. Note that the integral $I_1(a, b)$ is different from equations (17)–(18), because the argument of the delta function is not ξ but $\cos \xi$. In order to do the integration, we change variables, i.e. $\chi = b \cos \xi$, and thus $|\frac{d\xi}{d\chi}| = \frac{1}{\sqrt{b^2 - \chi^2}}$. Finally, we get

$$I_1(a, b) = \int_{-b}^b \frac{1}{\sqrt{b^2 - \chi^2}} \delta(a - \chi) = \begin{cases} \frac{1}{\sqrt{b^2 - a^2}} & |b| > |a| \\ 0 & \text{otherwise.} \end{cases} \quad (19)$$

Consider now a similar integral, but in the range from 0 to 2π :

$$J(a, b) = \int_0^{2\pi} d\xi \delta(a - b \cos \xi). \quad (20)$$

Change of variables from ξ to $\chi = b \cos \xi$ is not directly possible, since there are two values of ξ for each value of χ . The integration should be divided into two parts: the first from 0 to π and the second from π to 2π . Both cases give the same result, and so $J(a, b) = 2 I_1(a, b)$.

Let us next consider the double integral of the type

$$I_2(a, b) = \int_0^{2\pi} d\varphi_1 \int_0^{2\pi} d\varphi_2 \delta(a - b \cos(\varphi_1 - \varphi_2)). \quad (21)$$

In order to find its value we change variables to $\chi = (\varphi_1 + \varphi_2)/2$ and $\varphi = \varphi_1 - \varphi_2$, so that $d\varphi_1 d\varphi_2 = d\chi d\varphi$. Note that the integrand does not depend on χ , so integration over this variable gives 2π , while the remaining

$$I_2(a, b) = 2\pi \int_0^{2\pi} d\varphi \delta(a - b \cos \varphi) \quad (22)$$

already has been found.

Results given in equation (5) and equation (13) are obtained exactly in this way.

A2. Relation between probability distributions of L and L^2

In the next step, we will prove that the distribution of square of a random variable L , $p(L^2)$, is related to the distribution of L . We begin from the definition of the distribution function of the random variable

$$p(L^2) = \int dx g(x) \delta(x^2 - L^2), \quad (23)$$

where $g(x)$ is the probability density of finding the value x . We use relations $x^2 - L^2 = (x + L)(x - L)$ and assume that L is positive. With this we have

$$\delta(x^2 - L^2) = \delta((x - L)(x + L)) = \frac{1}{x + L} \delta(x - L)$$

and get

$$p(L^2) = \int dx g(x) \frac{1}{x + L} \delta(x - L), \quad (24)$$

which is equal to $\frac{1}{2L} p(L)$.

ORCID iDs

Jan Mostowski  <https://orcid.org/0000-0003-0887-7264>

References

- [1] Shankar R 2004 *Principles of Quantum Mechanics* (New York: Springer US)
- [2] Pitak A and Mostowski J 2018 *Eur. J. Phys.* **39** 025402
- [3] Atkins P W and Friedman R S 2011 *Molecular Quantum Mechanics* (Oxford: Oxford University Press)
- [4] Haken H and Wolf H C 2005 *The Physics of Atoms and Quanta: Introduction to Experiments and Theory* (Heidelberg: Springer)
- [5] Saari P 2016 *Eur. J. Phys.* **37** 055403
- [6] Malik M, Mirhosseini M, Lavery M P J, Leach J, Padgett M J and Boyd R W 2014 *Nat. Comm.* **5** 3115
- [7] Fickler R, Campbell G, Buchler B, Lam P K and Zeilinger A 2016 *PNAS* **113** 13642
- [8] Kuś M, Mostowski J and Pietraszewicz J 2019 *Phys. Rev. A* **99** 052112
- [9] Wigner E P 1959 *Group Theory and Its Application to The Quantum Mechanics of Atomic Spectra* (New York: Academic)

Supplementary material

S1. WKB APPROXIMATION

We will now discuss some properties of spherical harmonics and their WKB (semiclassical) approximation. Spherical harmonics $Y_{j,m}(\theta, \varphi)$ have the form $Y_{j,m}(\theta, \varphi) = \Theta_{j,m}(\theta) \exp(im\varphi)$. Functions $\Theta(\theta)$ satisfy equation:

$$\frac{d^2\Theta_{j,m}}{d\theta^2} + \frac{\cos\theta}{\sin\theta} \frac{d\Theta_{j,m}}{d\theta} + \left(j(j+1) - \frac{m^2}{\sin^2\theta} \right) \Theta_{j,m} = 0 \quad (\text{S1})$$

Substitution $\Theta_{j,m}(\theta) = \frac{1}{\sqrt{\sin\theta}} T_{j,m}(\theta)$ gives the following equation for $T_{j,m}(\theta)$:

$$\frac{d^2 T_{j,m}}{d\theta^2} + \left(\frac{\cos^2\theta}{4\sin^2\theta} + \frac{1}{2} - \frac{m^2}{\sin^2\theta} + j(j+1) \right) T_{j,m} = 0 \quad (\text{S2})$$

The Eq. (S2) has a form of the Schrödinger equation. The second derivative over θ plays the role of kinetic energy. Terms proportional to j^2 and m^2 are large in the semi-classical limit, while other terms are small. We will, therefore, skip these small terms. Then, the equation takes the form:

$$\frac{d^2 T_{j,m}}{d\theta^2} + \left(-\frac{m^2}{\sin^2\theta} + j^2 \right) T_{j,m} = 0 \quad (\text{S3})$$

and it is well suited for the WKB approximation. Let us note that the "kinetic energy" is positive only if θ is in the range between "classical turning points", i.e. $-\frac{|m|}{j} \leq \sin\theta \leq \frac{|m|}{j}$.

In order to apply the WKB approximation we look for the solution in the form:

$$T_{j,m} = \exp(iS(\theta)) + c.c. \quad (\text{S4})$$

Next we expand $S(\theta)$ into power series in j^{-1} and take into account that m is of the same order of magnitude as j . The leading term is proportional to j , the next one is j independent. Therefore, we get:

$$T_{j,m}(\theta) = \frac{1}{\left(\sin^2\theta - \frac{m^2}{j^2} \right)^{1/4}} \times \cos \left[j \left(\int \sin\theta' d\theta' \sqrt{1 - \frac{m^2}{j^2 \sin^2\theta'}} - \phi \right) \right]. \quad (\text{S5})$$

The integration should be taken from the smaller "classical turning point". This formula does not give the overall sign of the function, the normalization, nor the overall phase ϕ , these have to be found independently. The same formula as Eq. (S5), but restricted to $m = 0$ only, can be found in [10].

More careful analysis of the WKB approximation is given in [11]. This result is:

$$Y_{j,m}(\theta, \phi) \simeq (-1)^{j-m} \frac{\left[\frac{1}{\sin^2\theta - \frac{m^2}{j^2}} \right]^{1/4}}{\pi} \cos \left(\bar{J} \bar{S}_0 - \frac{\pi}{4} \right) e^{im\phi}, \quad (\text{S6})$$

$$\begin{aligned} \bar{S}_0 = S_0(0, m) &= \frac{m}{\bar{J}} \arccos \left(\frac{\frac{m}{\bar{J}} \cot\theta}{\sqrt{1 - \frac{m^2}{\bar{J}^2}}} \right) + \\ &+ \arccos \left(-\frac{\cos\theta}{\sqrt{1 - \frac{m^2}{\bar{J}^2}}} \right), \end{aligned} \quad (\text{S7})$$

where $\bar{J} = j + \frac{1}{2}$ due to limit of large j limit (or \bar{J} as well). This result is used in our numerical calculations. Differences between semiclassical and exact values are hardly visible for large j in the allowed region of θ .

S2. OSCILLATIONS OF THE CLEBSCH-GORDAN COEFFICIENTS

In this part we will provide an explanation of rapid oscillations of the CG coefficients seen in Fig. 3. Classical approximation cannot account for this effect, semi-classical methods have to be used. In order to show the mechanism of oscillations we will now use the formula expressing Clebsch-Gordan coefficients in terms of integrals over spherical harmonics:

$$\int Y_{j_1, m_1}(\theta, \varphi) Y_{j_2, m_2}(\theta, \varphi) Y_{J, M}^*(\theta, \varphi) \sin\theta d\theta d\varphi = \mathcal{K} \times \text{CB}(j_1, m_1, j_2, m_2; J, M), \quad (\text{S8})$$

where

$$\mathcal{K} = \sqrt{\frac{(2j_1+1)(2j_2+1)(2J+1)}{4\pi}} \begin{pmatrix} j_1 & j_2 & J \\ 0 & 0 & 0 \end{pmatrix}. \quad (\text{S9})$$

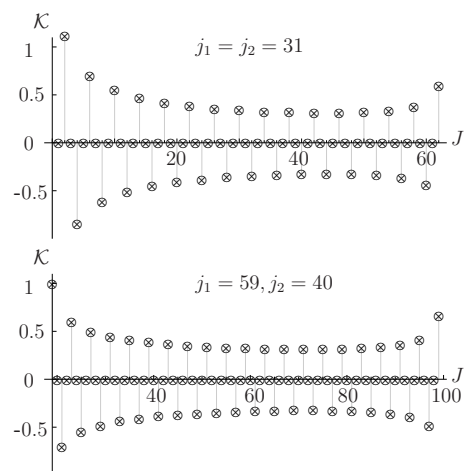


Figure S1: Coefficient \mathcal{K} for various settings of angular momenta (values on the plot).

The Eq.(S8) allows to determine the value of a CG coefficients only when the coefficient in front is not equal to zero. We are interested in the global features of the CG coefficients so this will not affect much the reasoning presented below. Some of the values of the coefficient \mathcal{K} are shown in Fig.S1. It is clear that these coefficients do not depend strongly on J , however, they influence signs of CG. The first integration over φ of the left hand side in the Eq.(S8) gives a nonzero value only if $m_1 + m_2 = M$. The second integration over θ will have to be examined more closely.

Fig. S2 gives the overall shape of the spherical harmonics, both exact and in the semi-classical approximation. The largest mismatch to the exact values occurs in the vicinity of the classical turning points, i.e., for $\sin \theta_0 \approx \sqrt{1 - \frac{m^2}{j^2}}$. There, strictly speaking, the semi-classical approximation is not valid. What is seen, however, is a certain trend, the semiclassical function is large in this region.

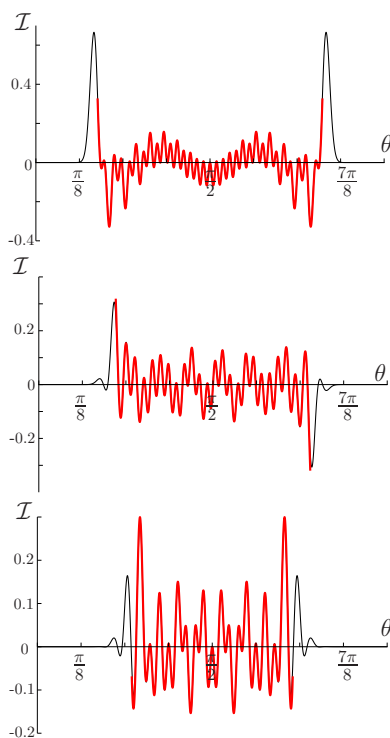


Figure S2: The integrand of Eq.(S8), marked by \mathcal{I} , as a function of angle θ given for $j_1 = j_2 = 31$ and $m_1 = 13, m_2 = 14$. The spherical harmonic results are shown by a black line, while their semi-classical counterpart results are shown in red. Parameters used for each plot, running from the left, are $J = 56, J = 43$ and $J = 36$. A perfect match between quantum and semiclassical functions is present for the whole θ -region until turning points $\theta_0(M/J) \simeq \arcsin(\frac{M}{J})$ and $\theta_0(M/J) = \pi - \arcsin(\frac{M}{J})$ are reached.

Let us now discuss a more complex case - the behavior of product of three semi-classical functions. With this, we will learn about the nature of the integrand, in the same way as in case of Eq.(S8).

It can happen that all three functions in Eq.(S8) have their turning points at about the same value of θ . In this case,

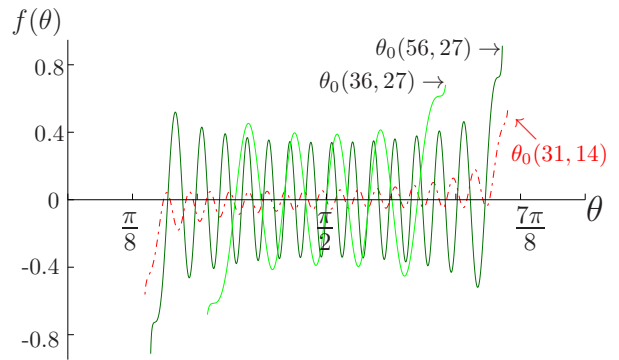


Figure S3: Functions contributing to integrand in the Eq. (S8), shown in the range of angles between their own turning points. The red, dashed line indicates the product of harmonics in the semi-classical approximation $f(\theta) = Y_{j_1, m_1}(\theta, 0) \times Y_{j_2, m_2}(\theta, 0)$ for the values $j_1 = j_2 = 31$ and $m_1 = 13, m_2 = 14$. In turn, both green lines show the behaviour of the $f(\theta) = Y_{J, M}(\theta, 0)$ function, which depends on the total angular momentum value J (values on the plot).

the value of the integral is determined by values of the integrand near the common turning points. One can also expect that the unusually large value of the integral occurs if all three functions are even (with respect to $\pi/2$). If one of the functions is odd and two other are even, than the values of the integral is unusually small - the contribution from one turning point is almost exactly cancelled by the contribution from the other turning point.

For better understanding, it is worth to have a look at the example in Fig. S3, where separate elements of the integrand are visualized. The red dashed line shows the behavior of the $Y_{j_1, m_1}(\theta, 0) \times Y_{j_2, m_2}(\theta, 0)$ in the allowed range of θ . Two green lines are semiclassical spherical harmonics $Y_{J, M}(\theta, 0)$ for two different values of J . Results of integration of the product of the red and one of the green functions are proportional to $CB_{j_1, m_1; j_2, m_2}^{J, M}$ coefficients in semiclassical approach, however, their semiclassical values dependent strongly on the position of the turning points $\theta_0(M/J)$. This will be noted later, in Fig.S4.

The spherical harmonics, exact and in the semiclassi-

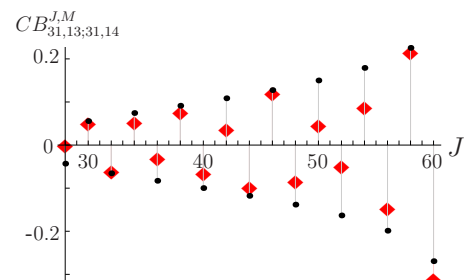


Figure S4: Clebsch-Gordan coefficients predictions obtained through integration of the left hand side of Eq.(S8) and dividing by factor \mathcal{K} . The black dots correspond to pure quantum results, while the red diamonds are semiclassical one. This example concerns $j_1 = j_2 = 31$ and $m_1 = 13, m_2 = 14$.

cal approximation, and also the \mathcal{K} factor, change sign when J changes by 1. This is probably the reason why the integral in Eq.(S8) changes its value when J is changed by 1, and explains the origin of the rapid oscillations of the CG coefficients. We should point out once more that this effect cannot be explained in the framework of the classical approximation.

Having all this information we can understand the key result of this section, namely behavior of the Clebsch-Gordan coefficients Fig.S4. It shows the computed values of CB coefficients, exact and in the semiclassical approximation for quantum numbers $j_1 = j_2 = 31$ and $m_1 = 13, m_2 = 14$. Oscillations of the coefficients are clearly seen.

Now, once again, we can state that the value and sign of the obtained results depend on the symmetry properties of the product of three spherical harmonics and on relative positions of their classical turning points.